The Mechanism of the Metal Cutting Process by the Sing'e-point Cutting Tool

The Mechanism of the Metal Cutting Process by the Sing'e-point Cutting Tool

Naoki YAMASAKI* and Fumio HASHIMOTO*

(Received June 30, 1962)

The mechanism of the metal cutting process by the single-point cutting tool with side cutting edge angle was geometrically investigated. Moreover the mean shearing stress, the shearing strain and others were calculated and the relationship among them was examined by means of applying the experimental results.

1. Introduction

The researches on the cutting mechanism have made remarkable progress particularly in these fifteen years. That is, Merchant[1] and Piispanen[2] have published the well-known orthogonal cutting theories, and the cutting mechanism has been investigated mostly as the orthogonal cutting operations. However most of the cutting operations at the practical laboratory works are the three-dimensional cutting, and single-point cutting tool is universally used.

We can find the researches about the three-dimensional cutting by Merchant[3], Stabler[4], Shaw[5] and Colwell[6], and these researchers referred to the application of the orthogonal cutting theory to the three-dimensional cuttitg. In 1952, Shaw examined the mechanism of the oblique cutting as the foundation of the three-dimensional cutting by putting together the researches of Merchant, Stabler and others, but not examined the influence of the rake angle in the case of the single-point tool.

Since the mechanism of the metal cutting by the single-point cutting tool is not sufficiently made clear, we examined the effective rake angle of the tool and the effective shear angle geometrically and led the formulae for calculating the mean shearing stress, the shearing strain and others in this report. Then we investigated the experimental results calculated with these formulae in comparison with the tendency about the orthogonal cutting.

2. The mechanism of the metal cutting process by the single-point cutting tool

We consider the cutting mechanism when the cylindrical specimen is cut by the single-point cutting tool forming the flow-type chip without built-up edge. As shown in Fig. 1, it is assumed that the shear occurs as the tool goes ahead, and the chip flows rubbing the rake face of the tool, same as the orthogonal cutting theory. Each character in Fig. 1 shows the following.

* Department of Mechanical Engineering, College of Engineering.

S=Feed (mm/rev.).

t=Depth of cut (mm).

C_e=End cutting edge angle (degree).

C_s=Side cutting edge angle (degree).

α_n=Rake angle measured in the plane perpendicular to the side cutting edge (normal rake angle) (degree).

α_e=Rake angle measured in the plane containing both the chip flow direction and cutting direction = (effective rake angle)(degree).

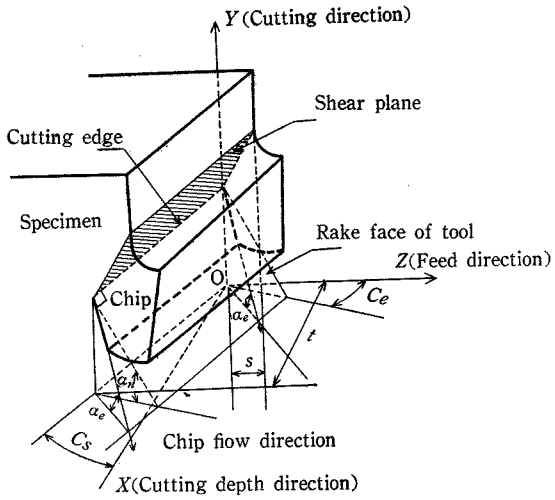

Fig. 1.

It is also assumed that the shape of shear plane is a parallelogram as shown in Fig. 2. Each character in Fig. 2 shows the following.

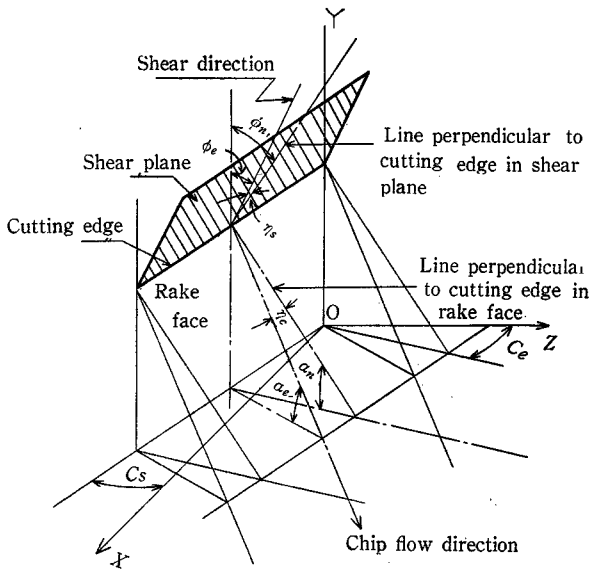

Fig. 2.

ϕ_n=Shear angle measured in the plane perpendicular to the side cutting edge (normal shear angle) (degree).

ϕ_e=Shear angle measured in the plane containing both the chip flow direction and the cutting direction (effective shear angle) (degree).

η_c=Angle between the line perpendicular to the side cutting edge and the chip flow direction on the rake face (degree).

η_s=Angle between the line perpendicular to the side cutting edge and the shear direction on the shear plane (degree).

Now, when the cutting ratio is indicated wite r_c, the next equation is given.

$$\tan\phi_n=\frac{r_c\cdot\cos\alpha_n}{1-r_c\cdot\sin\alpha_n} \qquad (1)$$

When the thickness of chip is indicated with S_c, r_c is represented by the next equation.

$$r_c=\frac{S\cdot\cos C_s}{S_c} \qquad (2)$$

When the inclination of the side cutting edge is indicated with α_b', the next equation is given.

$$\tan\eta_s=\frac{\tan\alpha_b'\cdot\cos(\phi_n-\alpha_n)-\tan\eta_c\cdot\sin\phi_n}{\cos\alpha_n} \tag{3}$$

The effective shear angle ϕ_e is indicated with the next equation.

$$\sin\phi_e=\left(\frac{\cos\eta_s\cdot\cos\alpha_e}{\cos\eta_c\cdot\cos\alpha_n}\right)\sin\phi_n \tag{4}$$

The shearing strain γ is represented by the next equation.

$$\gamma=\frac{\cot\phi_n+\tan(\phi_n-\alpha_n)}{\cos\eta_s} \tag{5}$$

These examinations are same as Shaw's examination about the oblique cutting.

In order to consider the force acting on the shear plane, we try to analyze the components of the cutting resistances. If the components of the cutting resistances F_t, F_c and F_s along the axis OX, OY and OZ in Fig. 1 and Fig. 2, can be measured by the experiment, F_t', the force along the side cutting edge on the rake face of the tool, F_c', the force perpendicular to the rake face, and F_s', the force perpendicular to the side cutting edge line on rake face, are given by the conversion of the Cartesian coordinates.[7] These F_t', F_c' and F_s' are given by the next equations.

$$F_t'=F_t\cos C_s\cdot\cos\alpha_b'+F_c\sin\alpha_b'-F_s\sin C_s\cdot\cos\alpha_b' \tag{6}$$

$$\begin{aligned}F_c'=&F_t(\sin C_s\cdot\sin\alpha_n-\cos C_s\cdot\sin\alpha_b'\cdot\cos\alpha_n)+F_c\cos\alpha_b'\cdot\cos\alpha_n\\&+F_s(\cos C_s\cdot\sin\alpha_n+\sin C_s\cdot\sin\alpha_b'\cdot\cos\alpha_n)\end{aligned} \tag{7}$$

$$\begin{aligned}F_s'=&F_t(\sin C_s\cdot\cos\alpha_n+\cos C_s\cdot\sin\alpha_b'\cdot\sin\alpha_n)-F_c\cos\alpha_b'\cdot\sin\alpha_n\\&+F_s(\cos C_s\cdot\cos\alpha_n-\sin C_s\cdot\sin\alpha_b'\cdot\sin\alpha_n)\end{aligned} \tag{8}$$

Then, in the plane perpendicular to the side cutting edge, F_{shn}, the force acting perpendicular to the shear plane and F_{shp}, the force acting along the shear plane are given by the next equations.

$$\begin{aligned}F_{shn}=&F_t(\sin C_s\cdot\cos\phi_n-\cos C_s\cdot\sin\alpha_b'\cdot\sin\phi_n)+F_c\cos\alpha_b'\cdot\sin\phi_n\\&+F_s(\cos C_s\cdot\cos\phi_n+\sin C_s\cdot\sin\alpha_b'\cdot\sin\phi_n)\end{aligned} \tag{9}$$

$$\begin{aligned}F_{shp}=&F_t(\sin C_s\cdot\sin\phi_n+\cos C_s\cdot\sin\alpha_b'\cdot\cos\phi_n)-F_c\cos\alpha_b'\cdot\cos\phi_n\\&+F_s(\cos C_s\cdot\sin\phi_n-\sin C_s\cdot\sin\alpha_b'\cdot\cos\phi_n)\end{aligned} \tag{10}$$

The shearing force acting along the shear plane is the resultant force of the force along the side cutting edge and the force acting along the shear plane perpendicular to the side cutting edge. This resultant force F_{sh} is given by the next equation.

$$F_{sh}=[(-F_t')^2+(F_{shp})^2]^{1/2} \tag{11}$$

Now, concerning the shear plane area, the width b and the height h are respectively given by the next equations.

$$b=\frac{t}{\cos C_s\cdot\cos\alpha_b'} \tag{12}$$

$$h=\frac{S\cdot\cos C_s}{\sin\phi_n} \tag{13}$$

Accordingly the shear plane A is represented by the following.

$$A=\frac{t\cdot S}{\cos\alpha_b'\cdot\sin\phi_n} \tag{14}$$

From above results, τ, the mean shearing stress in the shear plane and σ, the mean normal stress to the shear plane can be led as the next equations.

$$\tau=F_{sh}/A \tag{15}$$

$$\sigma=F_{shn}/A \tag{16}$$

3. The experiment and its result

In order to calculate the values of τ, σ and others, we made an experiment of cutting operation. The specimens, corresponding to S45C steel, were used after annealing one hour at 900°C, and mechanical property of them was the following. The yield

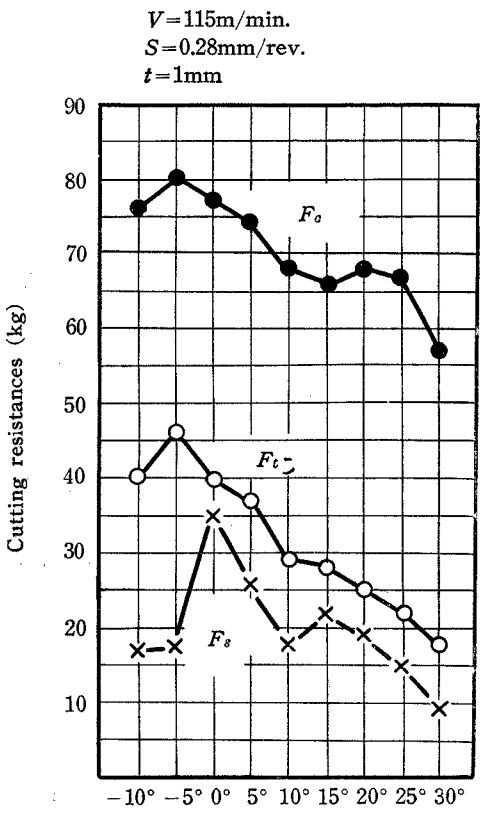

Fig. 3.

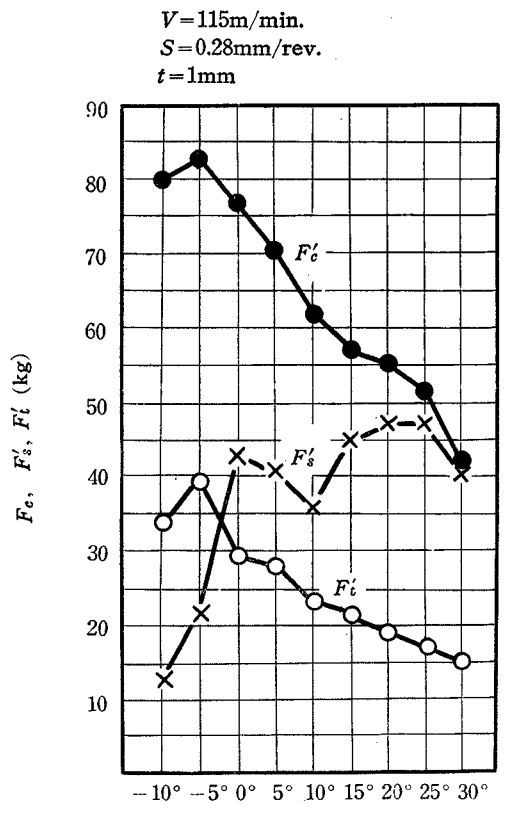

Fig. 4.

strength was about 34kg/mm², the tensile strength was about 56kg/mm² and BHN was 200. The dry cutting test was done by using the 6 feet length high speed lathe, and the typical values of the cutting resistances measured by the tool dynamometer are shown in Fig. 3. The tools were type S2 cemented carbide ones and shaped as (0°, Var., 6°, 6°, 15°, 15°, 0.5 mm).

While the three components of the cutting resistances are measured, F_t', F_c' and F_s' can be calculated by the equations (6), (7) and (8). Some of these values are shown in Fig. 4. Moreover we collected the chips in the course of experiments, and measured the thickness of them. In the actual cutting state as shown in Fig. 5, the cutting edge OA comes to $O'A'$ after once rotation of specimen by feed S, and the actual cutting area is the hatching area $A'B'EBA$. Then it is assumed that the cutting area is equal to $O''ACD$ and the length $O''A$, that is b, does not change with the cutting operation. Since the above assumption is approximately formed, the cutting ratio r_c can be calculated by the equation (2). The thickness of chips is shown in Fig. 6. Then ϕ_n, the shear angle in the plane perpendicular to the side cutting edge, can be calculated by the equation (1), and is shown in Fig. 7. The chip flow angle η_c is nearly

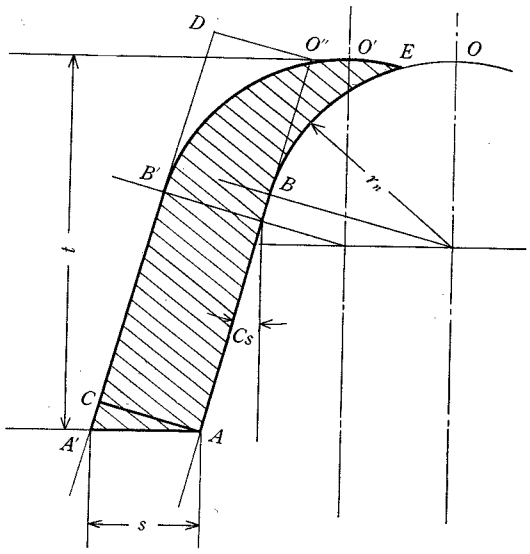

Fig. 5.
Cutting area (S=0.28mm/rev., t=1mm)

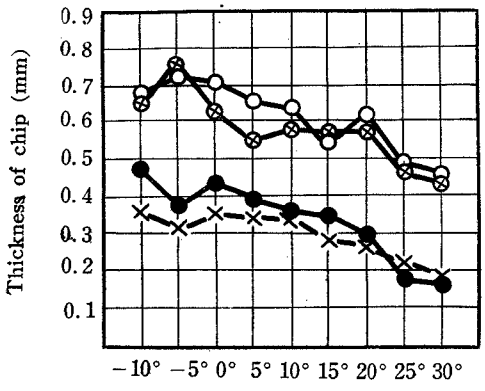

Fig. 6.
—○— S=0.28mm/rev., V=80mmin.
—⊗— S=0.28mm/rev., V=115m/min.
—●— S=0.12mm/rev., V=80m/min.
—×— S=0.12mm/rev., V=115m/min.

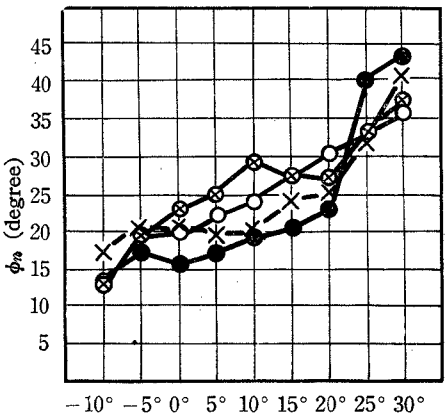

Fig. 7.
—○— S=0.28mm/rev., V=80m/min.
—⊗— S=0.28mm/rev., V=115m/min.
—●— S=0.12mm/rev., V=80m/min.
—×— S=0.12mm/rev., V=115m/min.

equal to η_{to}, that is, the direction of the frictional force on the rake face of the tool,[7] which can be calculated from the cutting resistances by the next equation.

$$\tan\eta_{to}=F_t'/F_s' \tag{17}$$

The values of η_{to} calcculated by the above equation are showe in Fig. 8. When η_{to} is equal to η_o, the effective rake angle α_e can be calculated by the next equation.

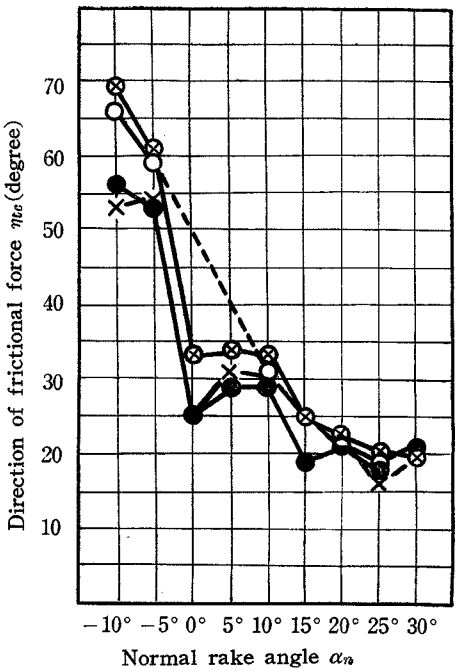

Fig. 8.

—○— $S=0.28$mm/rev., $V=80$m/min.
—⊗— $S=0.28$mm/rev., $V=115$m/min.
—●— $S=0.12$mm/rev., $V=80$m/min.
—×— $S=0.12$mm/rev., $V=115$m/min.

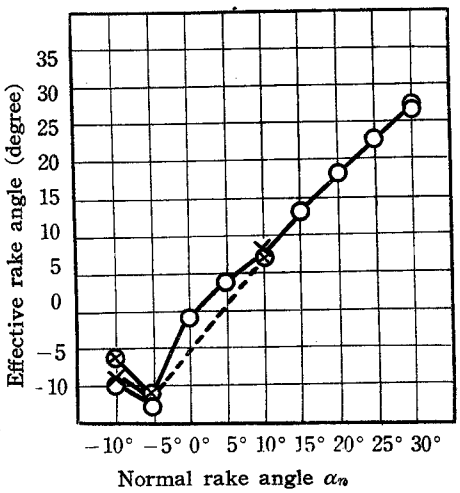

Fig. 9.

—○— $S=0.28$mm/rev., $V=80$m/min.
—⊗— $S=0.28$mm/rev., $V=115$m/min.
—●— $S=0.12$mm/rev., $V=80$m/min.
—×— $S=0.12$mm/rev., $V=115$m/min.

$$\sin\alpha_e=\sin\eta_o\cdot\sin\alpha_b'+\cos\eta_o\cdot\cos\alpha_b'\cdot\sin\alpha_n \tag{18}$$

The values of α_e are shown in Fig. 9. Then, as η_o is found, η_s can be calculated by the equation (3). Accordingly, ϕ_e is calculated by the equation (4), and shown in Fig. 10. The values of ϕ_e increase as the normal rake angle values, the feed values or the cutting speed values increase.

The shearing strain γ can be calculated by the equation (5), and is shown in Fig. 11. The values of γ decrease as the normal rake angle values, the feed values or the cutting speed values increase. According to these results, the same tendency is observed as the report about the orthogonal cutting.[8]

The shear plane area can be calculated by the equation (14) and is shown in Fig. 12. The shear plane area A decreases as the normal rake angle value increases or the cutting speed value increases. The mean shearing stress τ and the mean normal stress σ at the

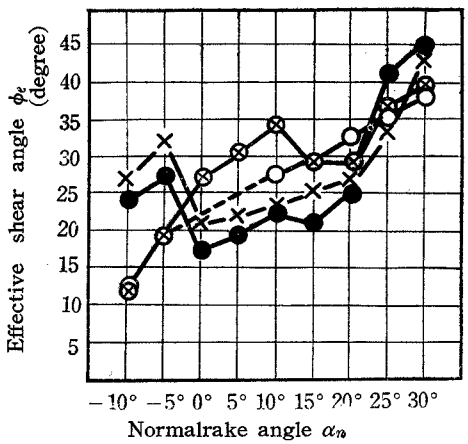

Fig. 10.

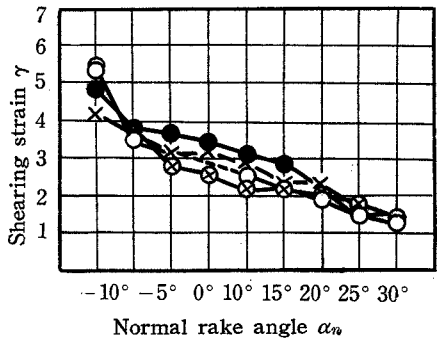

Fig. 11.

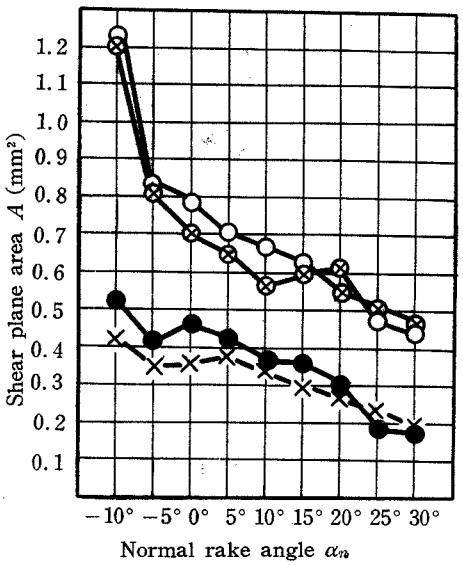

Fig. 12.

Common indications in Fig. 10~14

—○— S=0.28mm/rev., V=80m/min.
—⊗— S=0.28mm/rev., V=115m/min.
—●— S=0.12mm/rev., V=80m/min.
—×— S=0.12mm/rev., V=115m/min.

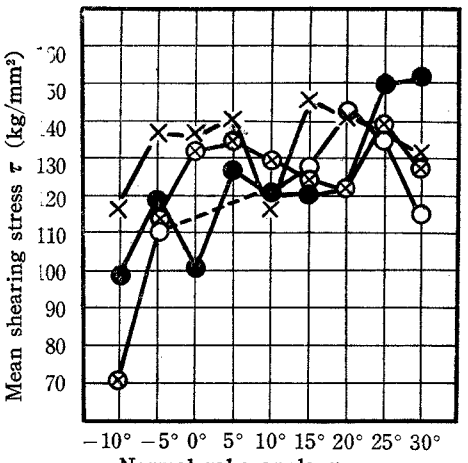

Fig. 13.

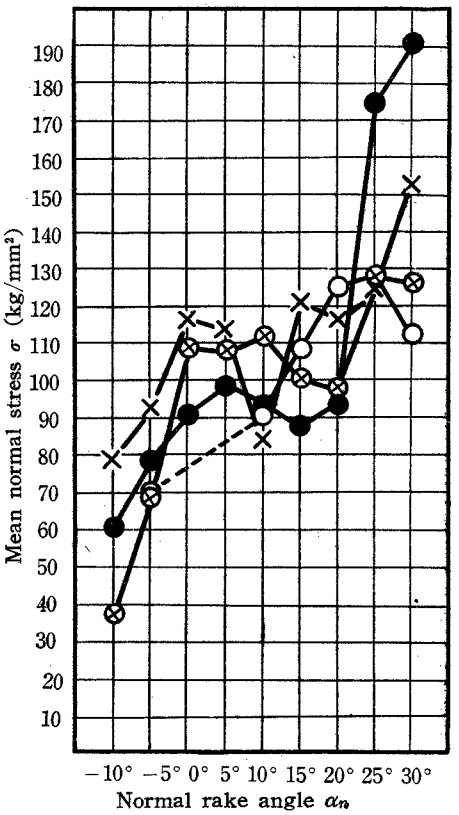

Fig. 14.

shear plane are calculated by the equations (15) and (16), and each value of them is shown in Fig. 13 and Fig. 14. The values of τ increase as the cutting speed values increase, and decrease as the feed values increase.

4. Consideration of the results

Considering our experimental results, we find that the mean shearing stress value τ is from 70kg/mm² to 150kg/mm². Since these values seem to be rather high, we will reconsider about the calculation of the shear plane area. While the nose radius of the

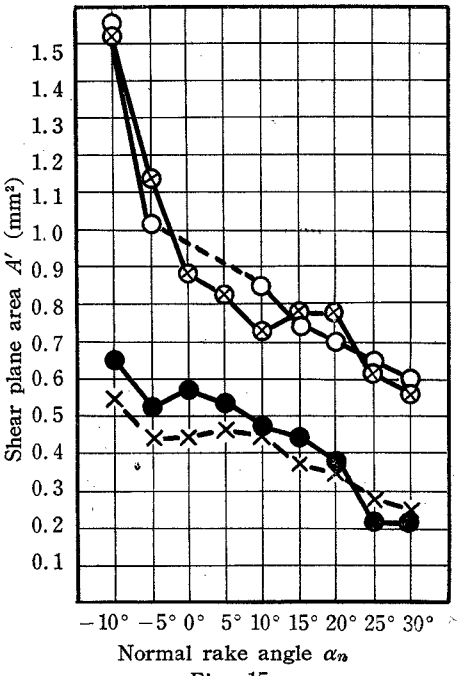

Fig. 15.

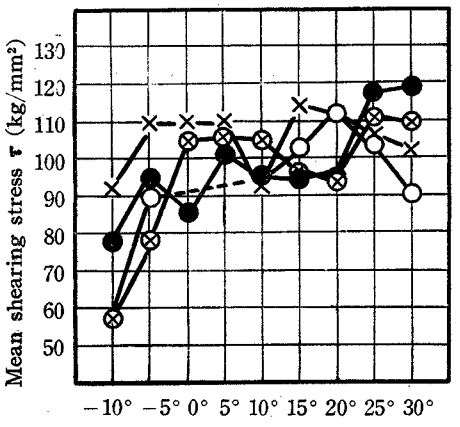

Fig. 16.

Common indications in Fig. 15~17

—○— S=0.28mm/rev., V=80m/min.
—⊗— S=0.28mm/rev., V=115m/min.
—●— S=0.12mm/rev., V=80m/min.
—×— S=0.12mm/rev., V=115m/min.

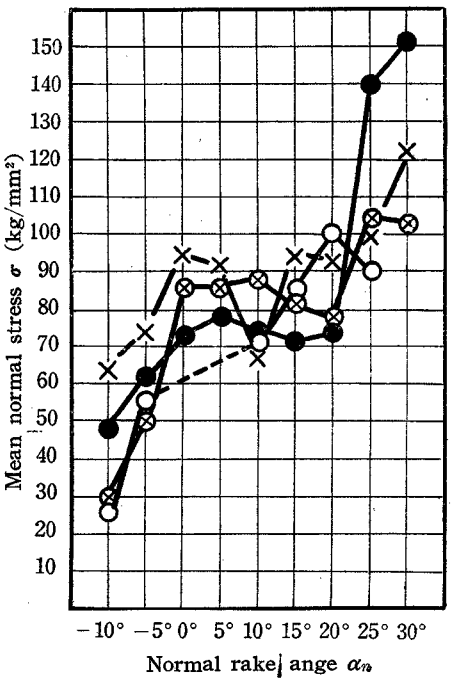

Fig. 17.

tool is 0.5 mm, and the depth of cut is 1 mm, as shown in Fig. 5, we made the influence of the nose radius to consider.

As the height of the shear plane area h, the value calculated by the equation (13) is used, and as the width b the value calculated by the equation (12) is not adopted. In Fig. 5, the length OBA, that is, from the end of the cutting edge to the contact point of the outside of the cutting depth is adopted as the width of the shear plane area. Namely, it is assumed that the shear plane area is the rectangular curved surface, of the height h and the width b'. Thereupon, when the nose radius is indicated with r_n, and r_n is smaller than t, b' is represented by the next equation.

$$b'=\frac{1}{\cos\alpha_b'}\left[\frac{t-r_n+r_n\cdot\sin C_s}{\cos C_s}+\frac{\pi r_n}{2}\left(1-\frac{C_s}{90^\circ}\right)\right] \tag{19}$$

The shear plane area A' calculater by the equations (13) and (19) is shown in Fig. 15. Then the mean shearing stress τ and the mean normal stress σ calculated by using the value of A' are respectively shown in Fig. 16 and Fig. 17. The relationship between the mean shearong stress τ and the shear plane area A' is plotted in Fig. 18. Similarly, the relationship between τ and the mean normal stress σ is plotted in Fig. 19 and the

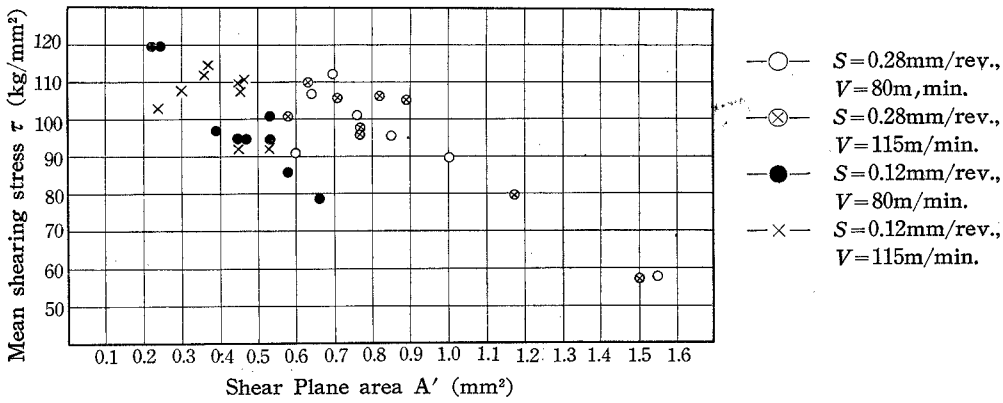

Fig. 18.

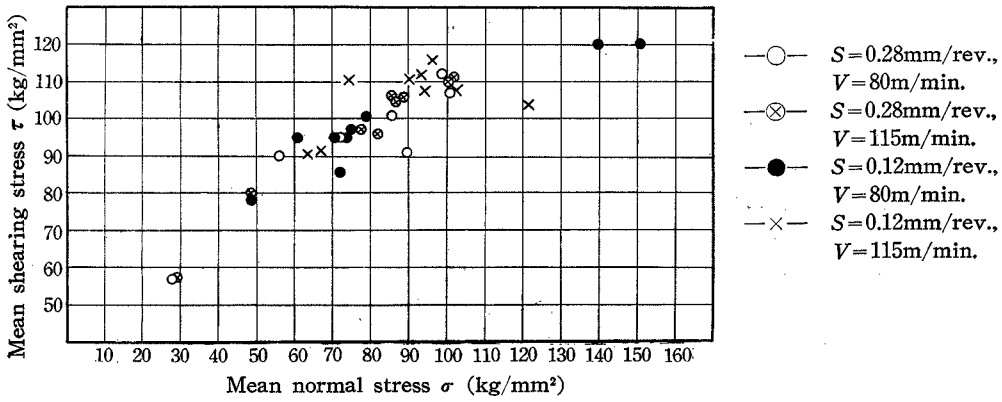

Fig. 19.

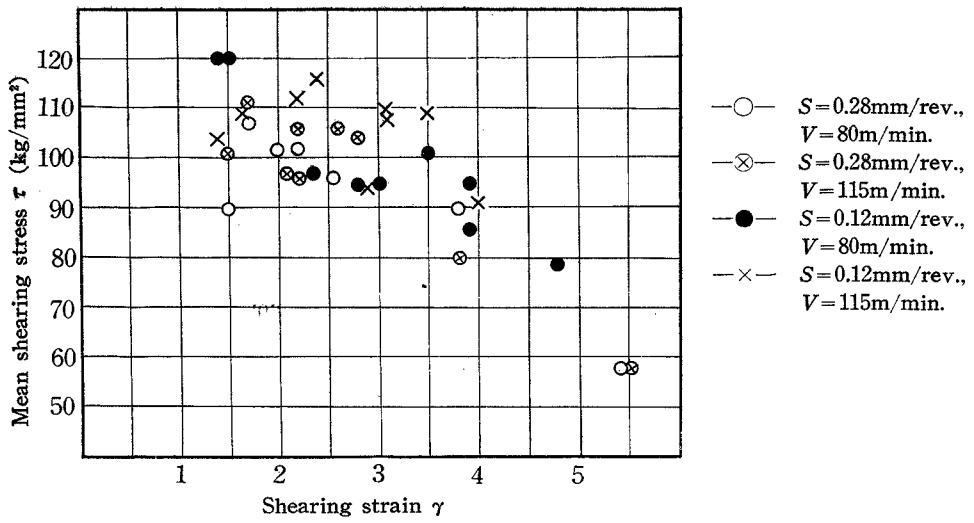

Fig. 20.

relation between τ and the shearing strain γ is plotted in Fig. 20.

After Shaw published the examination about the oblique cutting mechanism, Kececioglu[9] published, in 1960, the experimental results of the oblique cutting, that is, about the shear plane area, the compressive stress and the shearing stress in the shear plane and the shearing strain. Then he found that the shearing stress in the shear plane increased as the shear plane area decreased or as the compressive stress acting the shear plane increased, and decreased as the shearing strain increased. In the case of the single-point cutting tool, the same results as Kececioglu indicated are observed by Figs. 18, 19, and 20. Moreover, Opitz[8] presented the τ-γ diagram of the S35C steel in the orthogonal cutting operation, and reported that τ was from 70 kg/mm^2 to 110 kg/mm^2 and γ was from 1.5 to 7. On the other hand, Weber[10] reported that τ of the S45C steel in the cutting test was nearly equal to the tensile strength, 75 kg/mm^2. The specimen we used is the S45C steel and the value of τ is about from 60kg/mm^2 to 120kg/mm^2 as snown in Fig. 18. This value of τ seems to be approximately equal to the result of the orthogonal cutting. Namely the mean shearing stress in the shear plane, when the three-dimensional cutting is done by the single-point tool forming the flow-type chips, is nearly equal to the value in the case of the orthogonal cutting, and it can be said the above analysis is regarded as appropriate.

By means of thinking the plane containing both the chip flow direction and the cutting direction, the frictional force acting along the rake face of the tool can be treated in this plane. Moreover, the effective rake angle α_e and the effective shear angle ϕ_e can be treated in the same plane, and must correspond to the rake angle and the shear angle in the orthogonal cutting.

5. Conclusions

The mechanism of the cutting phenomenon with the single-point cutting tool has

been investigated by substituting for the simple cutting model. Then, as the experimental results, the following conclusions are led.

(1) In the case of the cutting with the single-point tool, the shearing strain and the shearing stress calculated from the experimental results are nearly equal to the result of the orthognal cutting theory.

(2) Namely, the mean shearing stress in the shear plane increases as the shear plane area decreases or as the mean normal stress to the shear plane increases, and decreases as the shearing strain increases.

(3) Concerning the S45C steel in the cutting test, the shearing strain in the shear plane is from 1.5 to 5.5, and the mean shearing stress is from 60kg/mm^2 to 120kg/mm^2.

Acknowledgement

Finally, we devote the hearty gratitude to Dr. Taketo Yokoyama, the emeritus professor of the University of Osaka Paefecture for his kind guidances.

References

1) M. E. Merchant: Mechanics of the metal cutting process I., II., J. App. Phys., Vol. 16, No. 5, No. 6, P. 267 (1945).
2) V. Piispanen: Theory of formation of metal chips., J. App. Phys., Vol. 19, No. 11, p. 876 (1948).
3) M. E. Merchant: Basic mechanics of metal-cutting process., J. App. Mech., Trans. ASME, Vol. 66, P. 168 (1944).
4) G. V. Stabler: The fundamental geometry of cutting tools., Proc. Inst. Mech. Engr., London, Vol. 165, P. 14 (1951).
5) M. C. Shaw, N. H. Cook, P. A. Smith: The mechanics of three-dimensional cutting operations., Trans. ASME, Vol. 74, No. 8, P. 1055 (1952).
6) L. V. Colwell: Predicting the angle of chip flow for single-point cutting tools., Trans. ASME, Vol. 76, No. 2, P. 199 (1954).
7) F. Hashimoto: The mechanism of three-dimensional cutting operations. (Part 2. Single-point cutting tool with side cutting edge angle.), J. Soc. Precis. Mech. Japan, Vol. 27, No. 8 (1961).
8) H. Opitz: Present-day status of chip-formation research., Microtecnic, Vol. 14, No. 4 (1960).
9) D. Kececioglu: Shear-strain rate in metal cutting and its effects on shear-flow stress., Trans. ASME, Vol. 80, No. 1 (1958).
10) G. Weber: Neuere Untersuchungen uber den Zusammenhang zwischen der Spanentstehung und dem Standzeitverhalten beim Drehen von Stahl mit Hartmetallegierungen., Stahl und Eisen, Bd. 78, Nr. 23 (1953).